GFZ
POTSDAM

Originally published as:

Schmidt, R., Petrovic, S., Güntner, A., Barthelmes, F., Wünsch, J., Kusche, J. (2008): Periodic Components of Water Storage Changes from GRACE and Global Hydrological Models. - Journal of Geophysical Research, 113, B08419

DOI: 10.1029/2007JB005363

Periodic components of water storage changes from GRACE and global hydrology models

R. Schmidt,[1] S. Petrovic,[1] A. Güntner,[1] F. Barthelmes,[1] J. Wünsch,[1] J. Kusche[1]

Abstract. We analyse spatio-temporal variations of surface mass anomalies induced by hydrological mass redistributions at the Earth's surface. To this end, we use a suite of global hydrological models as well as products from the Gravity Recovery and Climate Experiment (GRACE) satellite mission. As a novelty we identify dominating periodic patterns that are not restricted to the fundamental annual frequency and its overtones, using a method that combines conventional empirical orthogonal functions (EOF) analysis with a determination of sine waves of arbitrary periods from the principal components. We assess the significance of the derived spectra in view of correlated errors of the GRACE data by means of a Monte-Carlo technique. This allows us to create filtered GRACE time series including only the significant terms, which will serve for basin-specific calibration of hydrological models with respect to the dominant periodic water storage variations. The study reveals that besides dominating annual signals, semiannual (found only in a few basins), and also long-periodic waves in the range of 2.1 to 2.5 years contribute to periodic water storage variations. An interpretation and a preliminary explanation of these spectra is included. Comparisons of the spectra obtained from GRACE and global hydrological models exhibit in many river basins a systematic advance of the phases of annual terms of the hydrological models as compared to GRACE in the range of 1 to 6 weeks. This indicates deficiencies of the hydrological models w.r.t. runoff routing in the river network and/or water retention in lakes and wetlands.

[1]GeoForschungsZentrum, Potsdam, Germany

Copyright 2008 by the American Geophysical Union.
0148-0227/08/$9.00

1. Introduction

The main objective of the twin satellite Gravity Recovery and Climate Experiment (GRACE, *Tapley and Reigber* [2001]) is the detection of time-variable gravity signals related to mass redistributions at, on and below the Earth's surface caused by ongoing geophysical and climatological processes. The mission's actual sensitivity to processes such as continental hydrology (e.g. *Tapley et al.* [2004], *Wahr et al.* [2004], *Schmidt et al.* [2006]), post glacial rebound (e.g. *Tamisiea et al.* [2007]), changes in the polar ice sheets (e.g. *Velicogna and Wahr* [2006] , *Sasgen et al.* [2007]) and mass transport in the oceans (e.g. *Chambers et al.* [2004]) has been widely demonstrated in the recent past.

The ultimate goal is to allow for the quantification of the mass redistribution related to the individual phenomena to improve the modeling and understanding of the various processes. A still unresolved key question in this context is the signal separation of the individual contributions contained in the integral satellite gravity observations. As a preparatory step it is helpful to derive the characteristic spatio-temporal morphology of the surface mass anomalies traceable in time series of GRACE gravity models and for the processes to be detected.

To this end we propose an analysis method to derive such features from time series of surface mass anomalies in the space domain with a focus on periodic components due to continental hydrology. It combines a decomposition of the spatio-temporal signal using well-known Empirical Orthogonal Functions (EOFs) with a frequency analysis method which allows for the determination of harmonic (i.e. sine and cosine) waves with arbitrary periods. As basic result we obtain characteristic spectra of periodic mass variations contained in the GRACE data and in independent global hydrology models. Based on these it is possible to identify the hydrological components contained in the GRACE data. Further, the derived spatio-temporal behavior in terms of EOF modes give insight into the processes driving continental hydrology. Finally, the method allows for an effective filtering of the GRACE estimates of surface mass anomalies, i.e. it is possible to remove significant portions of spurious signals caused by the correlated GRACE model errors. This is an important task in the context of the actual usage of the GRACE data for the numerical validation and calibration of global hydrology models using GRACE. The proposed method is not limited to the examination of hydrological mass redistributions performed here and may therefore be valuable to further applications in other fields.

The paper is structured as follows. In section 2 we first present the input data for the analysis, which are time series of spatial grids of surface mass anomalies for 18 major river basins and over all continents (subsection 2.1). This is followed by a brief description of our methodology, i.e. we discuss the features of the EOF technique as relevant here (subsection 2.2) and give a description of the frequency analysis method used to derive the spectra (subsection 2.3). The accuracy of the GRACE-based spectra is assessed by means of a Monte-Carlo method based on correlated errors of the GRACE gravity models (subsection 2.4).

In section 3 and its subsections we present representative results for the EOF decomposition and the subsequent frequency analysis according to the characteristic periods that are found. This includes a discussion on the hydrological interpretation of the detected spectra, which are dominated by annual waves but also reveal some long-periodic fluctuations. For the latter comparisons to periodicities derived from climatological indices are carried out. In section 4 we derive filtered GRACE signals reconstructed from selected components (considered significant) and discuss the potential contributions of such data for calibrating hydrological models. Section 5 gives conclusions and an outlook.

2. Data and Methodology

2.1. Input Data and Preprocessing

Input data for our analysis are time series of spatial grids of surface mass anomalies from GRACE gravity fields and from water storage fields of various global hydrology models. These series are derived from time series of coefficients of spherical harmonics describing the gravity potential in both cases.

For GRACE such gravity potential coefficients are derived by the groups of the GRACE Science Data System (SDS) from the inter-satellite measurements, which are related to the gravity variations along the satellites' orbit (see e.g. *Reigber et al.* [2005]). In the following we use our own RL04 monthly model series generated at GFZ Potsdam (GFZ-RL04), considering the period 02/2003 - 12/2006. The series consists of 45 monthly gravity models, excluding June 2003 and January 2004 where no gravity field models are provided in GFZ-RL04 due to GRACE data gaps. In the period 07-10/2004 we use the constrained gravity field model versions provided by GFZ. These are regularized to compensate for the degraded ground track coverage due to the gradual entry/return into/from a 61(revolutions in)/4(sideral days) repeat orbit pattern in September 2004.

For hydrology four state-of-the-art global hydrology models are considered: the WaterGAP Global Hydrology Model (WGHM, *Döll et al.* [2003]), the H96 model [*Huang et al.*, 1996], the Land Dynamics (LaD) model [*Milly and Shmakin*, 2002], and the Global Land Data Assimilation System (GLDAS, *Rodell et al.* [2004]). The original hydrological data are provided in all four cases in terms of the total water storage variations on global grids. These are already available as monthly means, except for GLDAS where we use a series with a time step of 1 day. To obtain monthly sets for GLDAS as well, these maps are averaged. All the monthly maps are then expanded into sets of spherical harmonics describing the gravity potential (e.g. *Wahr et al.* [1998]).

This is done to allow for a common preparation of time series of grids of surface mass anomalies from GRACE and hydrological data sets. Each of the monthly spherical harmonic data sets is referenced to the individual long term mean for the period 2003-2006 to derive residual time-variable quantities. From these residual spherical harmonic coefficients time series of surface mass anomalies on 0.5°x0.5° grids are computed, applying the relations given by *Wahr et al.* [1998]. In order to suppress the artifacts in the GRACE data sets, known as *striping*, the Gaussian averaging filter in the spectral domain as described by *Jekeli* [1981] is used. For consistent treatment, it is applied to both the GRACE and the hydrological data sets.

To study a potential impact of the averaging radius on the obtained spectra different filter radii ranging from 300 to 750 km were used. However, as the results for the estimated periods and phases do not vary significantly with the filter radius we present in the sequel mainly results for the radius of 500 km which can be regarded as representative.

It is known that the Gaussian averaging filter is not optimal to suppress or remove the correlated errors of the GRACE-based surface mass anomalies and more refined methods (e.g. *Swenson and Wahr* [2006] or *Kusche*

[2007]) will be used in follow-on work. A more general concern in this context is the fact that any of the filtering techniques to reduce the correlated errors in the GRACE-based data introduces an attenuation of the signal amplitude. This is crucial when it comes to the actual application of the GRACE data in the course of hydrological model improvement or calibration where such an attenuation should be avoided. However, as we obtain consistent results with respect to the determination of signal periods and phases for different Gaussian averaging radii, the impact from the signal amplitude attenuation does not seem to be critical. Hence, the issue of an appropriate amplitude filtering is not considered further in this paper.

Since in this study the focus is laid on continental hydrology we extract from the global grids the data points located over land and data points located within 18 selected river basins worldwide (cf. Fig. 1). The size of the basins ranges from $5.9 \cdot 10^6$ km^2 for the Amazon to $85 \cdot 10^3$ km^2 for the Po basin, which is at the limit of the resolution of the GRACE mission. For reasons of space we present in detail only the results for four selected regions: the total continental area to study periodic mass variations induced by hydrology on the global scale; the Amazon basin as the world's largest drainage basin; the Ganges basin where in addition to annual terms also semiannual components are found, and the Mississippi basin which reveals an unconventional spectrum in the temporal mass redistributions compared to the majority of the investigated basins. Since the results with any of the hydrological models are in general very similar, we present mainly results of WGHM as a representative hydrological data set.

2.2. Empirical Orthogonal Functions (EOFs)

For studying the temporal characteristics of the spatial variability of surface mass anomalies from GRACE and the hydrology models, the well-known EOF analysis allows for a proper pre-processing of the data. We use conventional EOF analysis (e.g. *Preisendorfer* [1988] or *Wilks* [1995]), where decomposition into the mode-wise pairs of eigenvectors (evs) and associated principal components (pcs) is based on the signal variance-covariance matrix of the input data.

To get a first impression of GRACE's capability to trace mass redistributions caused by hydrology, simple comparisons of the evs and pcs can be performed. The idea is to look for equivalent features in the evs and pcs of corresponding modes. Finding such common features implies common causes of the observed data variability, since the input data series from GRACE and from the hydrological models are independent.

Figure 3 shows results for the first three modes for data points from WGHM and GRACE over the continents (a) and inside the Amazon basin (b) as two typical examples. Note that in both cases the evs from WGHM and GRACE have been normalized to make the results from the two sets comparable. To improve readability they were scaled by a factor of 1000. As it can be seen, one obtains a very good agreement of evs and pcs in the first two modes for both displayed cases. To illustrate the agreement of the first two modes correlation coefficients of the evs and pcs were computed, which are large for both the evs and pcs.

Similar results are obtained for the other basins and it is instructive to study the characteristics of the temporal variability of the spatial patterns described by the pcs.

2.3. Search for Arbitrary Periods in Principal Components

The results for the first two modes in Fig. 3 already indicate a dominance of annual periodicities. Therefore we look for periodic variations as they seem to dominate the temporal variability of the surface mass anomalies. Since the input data sets are driven by climatological processes that show variability in the signal amplitude, the signal phase and also the signal period both in space and time, we estimate all three quantities simultaneously.

Based on the ideas described in *Mautz and Petrovic* [2005], we estimate the amplitudes A_k, phase lags φ_k and frequencies $\omega_k = 2\pi f_k = 2\pi/T_k$ of the model consisting of terms

$$y_k(t) = A_k sin(\omega_k t + \varphi_k) \tag{1}$$

from the principal components $y(t)$ of individual dominant modes. For discrete data this problem can be transformed into a least squares adjustment problem with the observation equations:

$$\begin{aligned} y_i &= A_0 + Dt + \sum_{k=1}^{n} B_k \cos(\omega_k t_i) \\ &\quad + \sum_{k=1}^{n} C_k \sin(\omega_k t_i) + v_i, \qquad (i = 1, \dots N). \end{aligned} \tag{2}$$

where in addition to the amplitudes A_k and phase lags φ_k (contained in the B_k and C_k), also the unknown frequencies $\omega_k = 2\pi f_k = 2\pi/T_k$ (i.e. the periods T_k) and the trend parameter D are to be determined. The latter is estimated to avoid aliasing of secular signals into the periodic terms.

The major advantage of the approach proposed by eq. (2) is that the signal energy is mapped into few but representative frequencies, as it allows for the estimation of arbitrary periods in addition to the signal amplitudes and phases. This is in contrast to classical Fourier analysis where the signal energy is forced into a fixed basic period plus multiples of the associated basic frequency and only the signal amplitudes and phases are treated as unknowns. If this basic period differs from actual periods contained in the original signal (which is often the case when analyzing real world data), quite a large number of multiples of the basic frequency is needed to represent this signal. However, since in such a case some (or even all) terms included in the resulting frequency model do not correspond to the periodicities of the given signal, some (or even all) terms found by a Fourier-like approach will have only little or even no physical meaning and are not well suited for an interpretation. In this way, the apriori postulation of specific periods to be searched for is in general not very useful (cf. *Jochmann* [1993]) and the proposed non-standard approach offers an alternative to classical Fourier analysis.

Equation (2) represents a highly non-linear least squares problem for the determination of the periods $T_k = 2\pi/\omega_k$. In order to apply standard local optimization methods very accurate initial values for the to be estimated parameters are necessary. However, these can only be provided by global optimization methods, which require high computational effort (e.g. *Horst and Pardalos* [1995]). Since the observation equations (2) are non-linear only in periods, it is possible to eliminate the remaining unknowns, which are then computed after the determination of the periods. A reasonable strategy

based on a sequential algorithm is sketched in Fig. 2. The stability of the used sequential emulation of the common adjustment of all parameters was extensively investigated in (*Mautz* [2001], *Mautz* [2002]). Another critical point is the time-consuming global optimization step, especially in case of time series containig numerous epochs. However, in the present study, due to only 45 epochs, a simple systematic search performed well.

There are some consequences of the proposed data analysis strategy that need to be considered in the interpretation of the results in the later sections, and that can be easily veryfied by simulations. The first is that distinct temporal structures such as variations with different periods are not necessarily mapped by EOF into separate modes. This depends on the spatial patterns associated with these periodicities by the EOF. If the distinct temporal patterns belong to the same spatial pattern, then they must be mapped into the same mode. However, if the associated spatial patterns differ, then they are mapped into different modes.

The second is that temporal patterns with identical periods but with different phases and amplitudes can only be distinguished if they are connected to different spatial patterns and are consequently mapped into different modes. This means that it is possible to find several identical periods in the pcs, e.g. the annual, as long as these belong to different spatial patterns of variability. In the ideal case they may be attributed to distinct features of the underlying physical processes. On the other hand, it is possible to find different periods, e.g. the annual and the semiannual, in the principal component of the same mode. This means that both temporal patterns are associated with the same spatial variability pattern. This could be due to a non-harmonic behavior of the variability, thus requiring several harmonics of different periods to allow for a sufficient approximation of the given data. However, such behavior could also be implied by overlapping physical processes.

2.4. Accuracy Assessment of the Spectral Parameters from GRACE

In contrast to the hydrological data sets, where only little is known about the data accuracy, it is possible to assess the accuracy of the GRACE derived amplitudes, phases and periods. It can be done on the basis of the available GRACE gravity field model error estimates provided together with the gravity field models by the GRACE science data teams. In this study we use a Monte Carlo method for error propagation (*Gundlich et al.* [2003], *Kalos and Whitlock* [1988]), considering the spatial correlation of the GRACE gravity field errors.

Based on a scaled version of the full variance-covariance matrix of the monthly GRACE gravity model for August 2003 we create 200 spatial grids of noise in the surface mass anomalies for each of the 18 considered river basins. These grids are obtained through a rigorous error propagation of 200 realizations of correlated model errors via the Monte Carlo method. The noise grids are added to GRACE time series of grids of surface mass anomalies that are synthesized from the strongest periods found in the pcs of the EOF analysis. To this end we replace the original principal components of the modes of interest by the harmonic model from eq. (2) evaluated at the epochs of the input data using the amplitudes, periods and phases and then perform the inverse EOF transformation for these modes. In this way we obtain a filtered time series of 45 months of GRACE-based surface mass anomalies, containing a set of well-defined variations contamined by authentic noise. Applying the EOF and the frequency analysis to this data one can derive the standard deviations of the empirical distribution resulting for the amplitudes, periods and phases.

Since we do not know as yet whether the considered harmonic terms found in the pcs are really significant, the whole procedure must be repeated several times taking into account more or fewer terms (but the same noise data). This is done to avoid an over- or under-noising until the results confirm the assumption on the significant periods.

The applied GRACE model errors are currently considered as conservative estimates. The reason is that the scaling of the variance-covariance matrix is obtained through comparisons to the residual variability of monthly GRACE models in the space domain, which still contains plausible physical signal that is interpreted as error (see e.g. *Wahr et al.* [2006], *Schmidt et al.* [2007]). On the other hand, the results there, but also in *Horwath and Dietrich* [2006], reveal that the obtained spatial distribution of errors based on such rescaled covariance matrices may only represent propagated errors due to GRACE observation noise characteristics and the sampling geometry. Further important contributions due to so-called aliasing errors, visible in the spatial distributions of the residual GRACE signal, are seemingly not well represented by the rescaled covariance information at present. The investigation of the potential causes of and the assessment of these aliasing errors is still ongoing. Part of these errors seem to be induced by deficiencies in the background models e.g. describing short-term mass variations in the atmosphere and the oceans applied during the gravity recovery process (see e.g. *Reigber et al.* [2005]).

3. Application to Continental Grids and River Basins

As shown in *Petrovic et al.* [2007], the EOF analysis of grids with data points over the continents respectively inside river basins reveals that in the general case 80% and more of the total variability observed in GRACE and water storage of hydrology models is contained in the very first three to five modes. This is highlighted by Tab. 1, which shows the decrease of the contribution to the total signal as the mode number increases. It is also obvious from the plots shown in Fig. 3 (a) and (b). Hence, we limit the frequency analysis of the pcs and the accuracy assessment for the GRACE data to these lower modes.

Tables 2 to 9 summarize the periods detected in the pcs for the selected regions. In analogy to EOF, the results are tabulated in descending order, i.e. from the strongest to the weakest periodic component. This ranking is derived based on the percentual contribution of the harmonic component to the total variability of the input grid data, i.e. from the ratio $(var_{harm}/var_{total}) \cdot 100$ [%]. var_{total} denotes the variance of the original total signal (which includes noise) and var_{harm} is the signal variance of the spatial signal reconstructed from the harmonic components only. The latter is computed for each harmonic term as described in subsection 2.4 by replacing the original principal component $y(t)$ by the periodic $y_k(t)$ in the inverse EOF transformation.

For the GRACE-based results the accuracy assessment according to subsection 2.4 is displayed in Tab. 2 to Tab. 9 as well. For the interpretation of the errors of the amplitudes one has to note that the tabulated values have relative units, since absolute signal amplitudes are only given after the synthesis of the eigenvectors and principal components. However, the actual absolute amplitudes vary only with the relative amplitudes derived from the principal components multiplied by evs. In this way the

given relative error values hold for the errors of absolute amplitudes as well.

In the following interpretation of the detected periods it should be clear that they were determined from a finite data time interval. In this way, there is some uncertainty of the detected periodic terms with respect to an extrapolation to intervals outside the data period. This holds especially for parameters of signals with longer periods. One might therefore prefer to use a prefix like *quasi* for the estimated terms (e.g. quasi–annual). However, in a strict sense it is never justified to call systematic components estimated from an always finite data interval by their proper mathematical denominations. We therefore ignore such a distinction in the parameter names.

3.1. Detection of Annual Signals

The most dominant feature to be observed are annual periodic variations, which are found in virtually all of the investigated basins. In most of the areas considered in this study about 70-80% of the total variability seem to be represented by such annual waves. Only in the Mississippi basin we observe a weaker contribution of an annual term to the total variability (only about 40–45% cf. Tab. 8 and Tab. 9), which seems to be an exception.

The accuracy assessment of the GRACE-based results indicates a very good resolution of the annual terms, even for the results for the Mississippi basin. For the global case as well as for the Amazon or the Ganges basin the standard deviations of the derived annual periods and their phases are at the level of or even below one day. This is a relative error of about 0.2% for these parameters. The relative error of amplitudes is of the order of 1–2% for these basins. Even for the Mississippi the relative errors of the periods, phase and amplitudes of the annual term are still 0.9%, 3.4% and 4.7%, respectively.

As outlined in subsection 2.3 the detection of several annual signals in different modes is not surprising. This is caused by the spatial variability of the signal amplitudes, phases and periods inside the region of interest. For the example of the Amazon shown in Fig. 3 (b) these are well explicable by the distribution of the rainfall inside this basin. While the seasonality of rainfall is out of phase in the northern and southern Amazon, the basin average tends to be dominated by the southern Amazon because of its larger size [*Zeng*, 1999]. For the basin-average in the Amazon, the rainfall maximum is in February while the maximum of water storage is delayed by 1–2 months, peaking in March/April (*Zeng* [1999]; *Chen et al.* [2005]; *Güntner et al.* [2007])). This annual variation of total Amazon water storage is represented by the annual period in mode 1 with a phase of about 114 days (cf. Tab. 4). Spatially it coincides with the largest water storage variations focused in the eastern and south-eastern parts of the basin (Fig. 3 (b), mode 1) as a combined effect of rainfall-induced soil moisture and groundwater variations and seasonally varying storage in surface water (river and inundation areas). The latter component obtains a maximum in this lower part of the basin due to river flow convergence from upstream areas. The second annual period found in the analysis is due to the different phasing of water storage variations in the northern and southern part of the Amazon. These variations are induced by the rainfall seasonality governed by the seasonal north-south migration of the Intertropical Convergence Zone (ITC). As shown by *Güntner et al.* [2007] (Fig. 6 there), minimum water storage in the northern part is from December to February while it is from July-September in the southern part. This north-south distribution that roughly oscillates around the Amazon main channel is directly reflected in the annual period of mode 2 (cf. Fig. 3 (b)) and its corresponding phase of about 200 days (minimum in January, cf. Tab. 4).

In this way finding several annual periods associated to different spatial patterns inside one basin is not an artifact, but is a consequence of the processes governing the mass redistributions. Corresponding explanations may hold for other basins, but which are still to be studied in detail.

3.2. Detection of Semiannual Signals

Semiannual variations are only found in few investigated river basins. The contribution to the total variability is small, but can be determined significantly according to the obtained standard deviations. See for example the semiannual term for the Ganges shown in Tab. 6 and Tab. 7. We note that this semiannual term is found in the principal component of mode 1 and it thus has the same spatial variability pattern as the annual term. From the viewpoint of harmonic analysis, the detected semiannual signal could be regarded as a simple mathematical correction of the dominating annual term. It is therefore difficult to attribute the semiannual signal to some uniquely defined physical cause. Finding the semiannual term in a separate mode would exclude such an explanation based on overtones. On the other hand, several physical causes exist that may explain semiannual oscillations indeed. For example, they may be caused by a bimodal rainfall distribution within the year, such as known for the central tropical parts of the Congo or Nile basin. Indeed semiannual signals for the named basins are found both from GRACE and the hydrological models (not shown). Additionally, it should be noted that water mass variations on the continents are due to variations in different storage compartments, such as ground water, surface water and snow. These compartments are characterized by different water residence times and phases and may overlay in a complex way to give total mass variations. For example, in high-latitude basins such as the Ob and Yenisei river basins, there is the main storage peak in winter due to snow accumulation, and a second maximum (of much smaller amplitude) in summer caused mainly by surface water storage (*Güntner et al.* [2007]), presumbly leading to the semiannual periodicity found there. In this sense, the significant semiannual signal found for the Ganges basin may be caused by snow storage in the Himalayas and Central Asia to the North and Northeast of the basin which leads to a maximum of storage around February, fitting to the phase of the semiannual period in mode 1 (cf. Tab. 6 respectively Tab. 7). *Chowdhury and Ward* [2004] stress the importance of Himalayan snowpack and ice as a long-term and partly seasonal water reservoir for the Ganges basin.

3.3. Detection of Longer Term Periodic Signals

The results of the frequency analysis in Tab. 2 to 9 also show long-periodic variations in the range of 2 years and more. Similarly to the semiannual signals these represent only small contributions to the total variability, again at the level of a few percent. The obtained standard deviations for the GRACE-based estimates are much larger than for the annual and semiannual terms. For example, for the 2.1-yearly term found for the continental data set the error estimate for the period is about ± 1.2 months (relative error $\approx 5\%$) and for the phase about 0.6 month (relative error $\approx 2\%$). For the Amazon basin the period and the phase of the 2.5-yearly oscillation are more accurate than for the global case but with still much larger standard deviations than for the annual terms ($\sigma_{T=2.5y} \approx$ 27 days $\rightarrow$ relative error $\approx 3\%$, $\sigma_{\varphi=2.5y} \approx 19$ days $\rightarrow$ rel-

ative error $\approx$ 2%). For the long-periodic term in the Mississippi basin we obtain comparable values for the relative error of about 3.5% for both period and phase. For the amplitudes we also obtain a larger relative error than for the annual terms. For example for the global case, the Amazon, and the Mississippi the relative error of amplitudes is about 8%.

This illustrates the difficulties in clearly identifying such terms, in particular in view of the rather short period covered by GRACE so far. However, for several reasons they may be plausible nevertheless. First, it is possible to reproduce very similar values from longer time series (i.e. 12 years) of the hydrological models. For example, the long-periodic wave of about 2.5–2.8 years found on the global scale in GRACE and the hydrological models for the GRACE period (cf. Tab. 2 and 3) is also retrievable in hydrological models for the longer data period. The same holds for the long-perodic term found in the Amazon basin. An exception is the long-periodic wave of about 2.5 years in the Mississippi basin. That one is detected in the GRACE and the hydrology models only over the GRACE period, but not from the 12 years time series of the hydrological data. At present, potential causes of this very feature found for the Mississippi basin are unclear.

As a second argument for the plausibility of the detected terms may lie in the statistical significance of the results. Although the estimates of these terms are less accurate than those for the annual and semiannual signals, the accuracy assessment indicates a still significant detection of the long-term periodics. But also from the hydrological perspective such long-term variations are indicated. There are numerous studies reporting on quasi-biennial variability of hydro-meteorological variables in the range of 2–3 years, such as *Poveda and Mesa* [1997] for South-American rainfall records, *Rajagopalan and Lall* [1998] for precipitation in the U.S. or *Krokhin and Luxemburg* [2007] for Sibirian and eastern Asian precipitation and temperature which is related to ENSO (El Nino Southern Oscillation) variability. These authors also cite several studies with analogous results for various hydroclimatological variables worldwide. Given that precipitation is a main driving force for the hydrological cycle on the continents, similar variations can be expected for other water cycle components such as water storage and river discharge. *Güntner et al.* [2007] showed marked coherence of interannual spatio-temporal variations in water storage at the scale of continents with ENSO-related climate indices. For the Amazon basin, *Zeng et al.* [2008] showed large interannual variability of water storage composed of long-term decadal variations associated with major recharge or discharge periods of basin-wide water storage, superimposed by higher frequency variations at the annual or biannual scale which they relate with major El Nino or La Nina events. Similarly, for the Mississippi basin, *Zeng et al.* [2008] revealed considerable interannual variations at time scales shorter than 7 years that were related to drought and wet periods. For river discharge, *Labat et al.* [2005] and *Labat* [2008] summarized the dominant frequencies of interannual varitions in the discharge of large rivers worldwide and found good coherence with climate indices such as the Southern Oscillation Index (SOI) and the North Atlantic Oscillation (NAO).

Within this study we have made a preliminary analysis for some available climatological indices for the GRACE time span using our frequency approach. These include the Southern Oscillation Index (SOI) downloaded from the website of the Bureau of Meteorology of the Australian Government (http://www.bom.gov.au/climate/current/soihtm1.shtml), the Pacific Decadal Oscillation Index (PDO) from the website of the Joint Institute for the Study of the Atmosphere and Ocean (http://jisao.washington.edu/pdo/PDO.latest) and the North Pacific Oscillation Index (NPO) from the website of the National Center for Atmospheric Research (http://www.cgd.ucar.edu/cas/jhurrell/indices.data.html). In addition to a rich spectrum for short periodic terms (below 1 year), we find annual and long-periodic terms with 1.5-, 1.9- and 4.6-yearly periods, which do not agree too well with the long-period terms detected for hydrology in this study. This has to be investigated further.

3.4. Detection of Trend Signals

There are various studies that highlight GRACE's sensitivity to trend signals. These are induced by diverse processes like the melting of glaciers in the polar regions (e.g. *Velicogna and Wahr* [2006]), post-glacial rebound (e.g. *Tamisiea et al.* [2007]) or the mass redistributions caused by the Sumatra-Andaman earthquake (e.g. *Han et al.* [2006]). An indication of the detection of such signals with GRACE and the presence of comparable secular changes in continental hydrology may be given by the plots of mode 3 for the global grids shown in Fig. 3 (a). In the context of the determination of the periodic terms considered here, we always estimate trend signals simultaneously (cf. eq. (2)) to avoid aliasing in the estimates for the periodic terms. However, we leave the investigation and interpretation of these trends for a later study.

4. Reconstruction of Filtered GRACE Time Series of Surface Mass Anomalies

Filtering of the GRACE data, in the sense of a signal-noise separation, is an important task for the actual usage of the GRACE data for the calibration of geophysical and climatologically driven models like global hydrology models. Using the approach to construct the harmonic signals described in subsection 2.4 it is possible to create such filtered GRACE time series of surface mass anomalies. To this end we use the harmonic components of the pcs for the EOF synthesis that 1) are found also in the hydrology data and 2) which are significant according to the accuracy assessement.

In this context the detection respectively the presence of two or more nearby periods (like the annual), that might look like doublet periods, may be of some concern. Recalling the features of the EOF model to describe the variability of spatial data (cf. subsection 2.2 and 2.3), finding nearby periods is only possible for pcs of different modes. That is to say, harmonic oscillations with nearby periods in the EOF model are only possible if they are associated to different spatial variability patterns (or evs, respectively). This distinction originates from the input data, i.e. from given variations of the period, the phase and the amplitude inside the region of interest.

Let us for simplicity first assume that there are only two periodic terms with identical periods, coming from two different modes, i.e. associated with two different patterns. It can be shown using very simple mathematics that the EOF-based model of the spatial data variability can be transformed into a point-wise model which associates to each point inside the considered region a one-dimensional wave with the given period. For each point the amplitude and phase depend on its position inside the region. This transformation can be performed in both directions exactly.

If we additionally allow a small variation of the period

inside the region, i.e. from point to point, there is no exact transformation between the two described representations. However, having in each grid point an oscillation, all of them having nearby periods and arbitrary amplitudes and phases, it is possible to approximate all of them, i.e. over the whole of the region of interest, by two or more periodic terms and associated patterns in the EOF model. The transformation in the other direction is also approximate. It is clear that at the level of the point-wise data real doublets are never possible.

A main result of the present study is that *only* two periodic waves and their associated patterns are sufficient to approximate the point-wise variations of periods, phases and amplitudes of dominating annual oscillations inside the considered regions.

This can be easily demonstrated. For the global case, we reconstruct maps of surface mass anomalies for only the two relevant periods for GRACE and WGHM. Then, to the resulting 45 grids of surface mass anomalies we fit the model based on equation (2) to each grid point, i.e. we estimate for each data pixel an amplitude, period and phase. In such a way it is possible to represent approximately 99.7% of the variability contained in the two region-wide annual waves by one single amplitude, period and phase at each location. Global plots of the estimated amplitudes, periods and phases (not presented) show the coincidence with the expected regions of surface mass variations from hydrology, and the signal phases correlate well with the principal climatological zones of the Earth. To illustrate the agreement of the reconstructed data for GRACE and WGHM we display the differences of derived annual periods and phases in Fig. 4 (a) and (b), respectively. For the annual periods it can been seen that the agreement is within $\pm$ 4 days in most regions of the continents, which is quite remarkable.

For the phases the agreement between GRACE and WGHM, displayed in Fig. 4 (b), is at the level of $\pm$ 1 month. A closer investigation of the orange to red areas in Fig. 4 (b) indicates a systematic offset of about 1 month in many regions of the continents. That is to say, the variations of surface mass anomalies from WGHM are seemingly about 1 month ahead of the GRACE estimate in these regions. There are also regions where the GRACE phases are ahead of WGHM (green to blue areas in Fig. 4 (b)). However, a large portion of these may be explained by instabilities for the phase estimates from GRACE and WGHM at the border of the catchment areas and in the areas where the signal amplitude reduces below the GRACE sensitivity (e.g. the deserts in Northern Africa, Arabia, the Middle East, Western China and Mongolia). Together with potential inaccuracies of the hydrological models in such areas an unambiguous interpretation of the differences between the phases derived from GRACE and hydrological data in these regions is difficult. On the other hand, since an advance of the signal phase of the annual terms is detectable for all the tested hydrology models in common regions, it seems to be a systematic feature. For illustration, Tab. 10 shows the estimates for the first two annual terms for the Amazon basin for the LaD, H96 and GLDAS hydrology models. Comparing with the GRACE and WGHM results in Tab. 4 and Tab. 5, respectively, the offsets GRACE minus hydrology model are always positive and range from 8 (WGHM) to 29-36 days (LaD, H96 and GLDAS) in that basin. The smaller difference for WGHM could result from the explicit modeling of surface water storage which is not included in the other considered models.

In a next step we extend the harmonics used for the synthesis to additional terms that can be considered plausible and/or significant. As a typical example we use the Amazon, where at least the first four harmonic terms displayed in Tab. 4 fullfill this criteria. The first and the third column in Fig. 5 show the resulting 12 monthly grids for the year 2005 from these four terms, i.e. two annual plus a 2.5-yearly and a 1.3-yearly signal. These explain 92% of the total variability of the input data. As discussed in section 3 the reconstructed grids clearly display the variations induced by the rainfall seasonality governed by the seasonal north-south migration of the ITC.

In the second and the fourth column of Fig. 5 residual mass anomalies are shown. These are derived as the difference of the original grid of surface mass anomalies of each month minus the reconstructed signal. The distribution of the residual signal is quite interesting. It reveals a north-south oriented pattern, which resembles the typical feature of the correlated errors of the GRACE-only gravity models. This result gives indication that a proper signal-noise separation is achieved by this approach.

It is clear that the residual signal may still contain traces of hydrological signal and cannot be interpreted as pure errors. However, since the amplitude of the residual signal is small, it explains only 8% of the total variability which includes noise as well, the potentially neglected hydrological signals should be very small. Vice versa, the reconstructed signal from the selected harmonic terms may also contain some small portions of the error signals. However, the accuracy assessment shows, that the relative contributions of errors in the derived dominating terms are much smaller than in the residual part. In this way the construction of filtered surface mass anomalies from the dominating terms will be useful for the validation and calibration of hydrological models.

For illustration of that we create basin averages of surface mass anomalies in the Mississippi for the original Gaussian grids and for the reconstructed signal (cf. Fig. 6). For the latter we choose the first two dominating terms from Tab. 8 (i.e. the annual term and the 2.5-yearly one) according to the above criteria on significance and plausibility. The basin averages of the surface mass anomalies are computed as weighted mean over all data points inside the river basin. Figure 6 (a) and (b) depict the original time series of the (Gaussian averaged) basin averages from GRACE (dashed line in Fig. 6 (a)) and WGHM (dash-dotted line in Fig. 6 (b)). These curves exhibit some general agreement, but also substantial differences, e.g. at the beginning of year 2003, where GRACE observes larger signal variations that are not present in the WGHM data. In addition, the variations in GRACE have an overall larger amplitude than the corresponding variations in WGHM.

The reconstructed signals for GRACE is shown in Fig. 6 (a) as solid line with circles and for WGHM in Fig. 6 (b) as solid line with triangles, respectively. The filtered WGHM signal is computed from the first two harmonic terms listed in Tab. 9. After a scaling of the amplitude of the reconstructed WGHM curve, to match the amplitude of the filtered GRACE signal, we obtain the curves displayed in Fig. 6 (c). As it can be seen the rescaled version of the WGHM-based time series and of the GRACE-based data exhibits a fairly good agreement except for a phase bias of about 1.4 months, the feature which was already highlighted before. To verify that this is not specific to WGHM we also look at the other hydrology models and obtain: GRACE - GLDAS $\approx$ 0.1 months, GRACE - H96 $\approx$ 0.7 months and about 1.3 months for GRACE - LAD. Suppressing the phase bias for the WGHM case by shifting the rescaled WGHM curve onto the GRACE filtered signal curve we get Fig. 6 (d) which reveals an almost perfect agreement of the two

data sets after these transformations.

These results are even more remarkable as in the Mississippi basin the given changes in surface mass anomalies are far less dominated by harmonic variations (the two strongest terms only explain some 55% of the total variability) than in the case of the majority of the other basins where even better results can be obtained. In this way the results for the Mississippi clearly demonstrate the capability of the proposed procedure to efficiently extract patterns of harmonic mass variability, which will serve in turn for the basin-specific calibration of hydrological models with respect to the dominant periodic variations of water storage.

5. Conclusions and Outlook

In this contribution we have derived characteristic spectra of periodic respectively quasi-periodic surface mass variations induced by continental hydrology observable in time series of GRACE gravity and global hydrology models. To this end we apply a combined EOF and frequency analysis method, where the latter allows for the determination of arbitrary periods from the temporal patterns of the derived EOF modes. This constitutes an interesting alternative to conventional, Fourier-based frequency analysis of data, as it may allow for a more adequate description of time variability contained in geophysical data. For the GRACE-based spectra we perform an accuracy assessment using available GRACE error estimates via a Monte-Carlo simulation.

Concerning the characteristic features of hydrologically induced mass redistributions, we can conclude that these are dominated by annual variations and that they are accurately determined by GRACE. Such terms explain about 60% to more than 90% of the total data variability, which are well determined in the GRACE data. The relative errors of the annual periods and phases are small and seem to be at the level of about $\pm$ 1 day for most of the basins.

For the phases of the annual terms we observe a systematic delay between GRACE-based surface mass anomalies and the hydrology models. Depending on the model and the region, the phases from the hydrological models are about 1 to 6 weeks ahead of the GRACE estimate. This difference may point to systematic deficiencies in hydrological modeling. For example, water storage in surface water bodies will cause a delay of freshwater runoff from the continental areas. However, processes of runoff routing in the river network and lake/wetland water retention are not taken into account by the hydrological model versions used in this study, except for WGHM.

The fact of finding several annual terms (but associated with different spatial patterns) per region is a consequence of the spatial variability of the underlying processes and is not an artifact of the method. This could be clearly demonstrated for the Amazon, where the detected two annual terms are well explainable by the temporal distribution of the rainfall and its migration with the Intertropical Convergence Zone. For other basins similar explanations still have to be investigated.

Semiannual terms do not play a significant role, at least on the global scale. On the level of drainage basins only in a few regions, e.g., for the Ganges, the Nile, the Congo, and the Ob, semiannual variations are traceable. However, since their contribution to the total variability is in general small, a clear separation as for the dominant annual terms is difficult. Potential hydrological causes of such signals may originate from a bimodal rainfall distribution in tropic areas, but could also arise from a complex overlay of mass variations in the different storage compartments such as ground water, surface water and snow. In the case of the Ganges the influence of changes in the Himalayan snowpack is speculated, but this has to be investigated further.

Moreover long-periodic signals with periods of 2 years and more are observed. As for the semiannual signals these provide only very small contributions to the total variability making a detection difficult. In connection with the short data period covered by GRACE so far, a separability of such features may be limited. This is clearly reflected in the error estimates, which are larger than those of the annual and seminannual terms.

On the other hand, in many cases the detected long-periodic signals can be still considered significant and thus may represent plausible hydrological signals nevertheless. In various contributions to the hydro-climatological literature several authors discuss such variations, which may be related to long-term mass redistributions caused be climatological variations like the El Nino Southern Oscillation. It seems that such signals are implicitely contained in the hydrological models via the climatological input data, as we retrieve quite comparable long-term periods from short and long term (12 years) model data series. In addition, these are consistent with the estimates obtained from GRACE for many basins, which could be seen as another hint to long-term mass redistributions. However, from preliminary comparisons with spectra derived from available climatological indices we cannot infer a definite connection to such climatological variations.

Finally, in combination with the results from the accuracy assessment of GRACE-based spectra, it is possible to derive filtered GRACE surface mass anomaly data. These are reconstructed via the inverse EOF transformation where the original principal components are replaced by harmonic terms that 1) are found consistently also in hydro-climatological models and that 2) are significant according to the error estimates. Such anomaly data, revealing a distinct signal-noise separation, will be of benefit for calibration and validation purposes of hydro-climatological models. As the method is not restricted to the presented study case of hydrology, it may be of general interest for a wide set of geophysical applications in the context of an assimilation of GRACE-based surface mass data.

Acknowledgments. The German Ministry of Education and Research (BMBF) supports these investigations within the geoscientific R+D programme GEOTECHNOLOGIEN "Erfassung des Systems Erde aus dem Weltraum" under grant 03F0424A. We thank P.C.D. Milly, Y. Fan and H. van den Dool, M. Rodell as well as P. Döll and J. Alcamo for providing the LaD, H96, GLDAS and WGHM model data, respectively. Thanks also go to D.W. Pierce for his Empirical Orthogonal Functions (EOF) software, and two anonymous reviewers whose constructive remarks helped us to improve the manuscript.

References

Chambers, D. P., J. Wahr, and R. S. Nerem (2004), Preliminary observations of global ocean mass variations with GRACE, *Geophys. Res. Lett.*, *31*, L13310, doi: 10.1029/2004GL020461.

Chen, J. L., M. Rodell, C. R. Wilson, and J. S. Famiglietti (2005), Low degree spherical harmonic influences on Gravity Recovery and Climate Experiment (GRACE) water storage estimates, *Geophys. Res. Lett.*, *32*, L14405, doi: 10.1029/2005GL022964.

Chowdhury, R., and N. Ward (2004), Hydro-meteorological variability in the greater Ganges-Brahmaputra-Meghna

basins, *Int. J. Climatol.*, *24*, 12.
Döll, P., F. Kasper, and B. Lehner (2003), A global hydrological model for deriving water availability indicators: model tuning and validation, *J. Hydrol.*, *270*, 105–134.
Gundlich, B., K.-R. Koch, and J. Kusche (2003), Gibbs sampler for computing and propagating large covariance matrices, *Journal of Geodesy*, *77*(9), 514–528.
Güntner, A., J. Stuck, S. Werth, and Döll, P. and Verzano, K. and Merz, B. (2007), A global analysis of temporal and spatial variations in continental water storage, *Water Resour. Res.*, *43*, W05416, doi:10.1029/2006WR005247.
Han, S.-C., C. K. Shum, M. Bevis, C. Ji, and C.-Y. Kuo (2006), Crustal Dilatation Observed by GRACE After the 2004 Sumatra-Andaman Earthquake, *Science*, *313*, 658–662, doi:10.1126/science.1128661.
Horst, R., and P. M. Pardalos (Eds.) (1995), *Handbook of Global Optimization*, *Nonconvex Optimization and Its Applications*, vol. 2, Kluwer Academic Publishers, Dordrecht.
Horwath, M., and R. Dietrich (2006), Errors of regional mass variations inferred from GRACE monthly solutions, *Geophys. Res. Lett.,* , *33*, L07502, doi:10.1029/2005GL025550.
Huang, J., H. M. van den Dool, and P. K. Georgakakos (1996), Analysis of model-calculated soil moisture over the United States (1981-1993) and applications of long-range temperature forecasts, *J. Climate*, *9*, 1350–1362.
Jekeli, C. (1981), Alternative Methods to Smooth the Earth's Gravity Field, *Tech. Rep. 327*, The Ohio State University.
Jochmann, H. (1993), Die modifizierte Fourier-Analyse einer zweidimensionalen Bewegung, *ZfV (Zeitschrift f. Vermessungswesen)*, *118*(1), 6–10.
Kalos, M. H., and P. A. Whitlock (1988), *Monte Carlo methods*, Wiley, New York.
Krokhin, V. V., and W. M. J. Luxemburg (2007), Temperatures and precipitation totals over the Russian Fast East and Eastern Siberia: long-term variability and its links to teleconnection indices, *Hydrology and Earth System Sciences*, *11(6)*, 1831–1841.
Kusche, J. (2007), Approximate decorrelation and non-isotropic smoothing of time-variable GRACE-type gravity field models, *Journal of Geodesy*, doi:10.1007/s00190-007-0143-3.
Labat, D. (2008), Wavelet analysis of the annual discharge records of the world's largest rivers, *Advances in Water Resources*, *31*, 1.
Labat, D., J. Ronchail, and J. L. Guyot (2005), Recent advances in wavelet analyses: Part 2 - Amazon, Parana, Orinoco and Congo discharge time scale variability, *J. Hydrol.*, *314*, 1-4.
Mautz, R. (2001), Zur Lösung nichtlinearer Ausgleichungsprobleme bei der Bestimmung von Frequenzen in Zeitreihen, Ph.D. thesis, Deutsche Geodätische Kommission, Series C., No. 532, 87 pp.
Mautz, R. (2002), Solving Nonlinear Adjustment Problems by Global Optimization, *Bollettino di Geodesia e Scienze Affini*, pp. 123–134, Vol 61, No. 2.
Mautz, R., and S. Petrovic (2005), Erkennung von physikalisch vorhandenen Periodizitäten in Zeitreihen, *ZfV (Zeitschrift f. Geodäsie, Geoinformation und Landmanagement)*, *130*(3), 156–165.
Milly, P. C. D., and A. B. Shmakin (2002), Global Modeling of Land Water and Energy Balances. Part I: The Land Dynamics (LaD) Model, *J. Hydrometeor.*, *3*, 283–299.
Petrovic, S., R. Schmidt, J. Wünsch, F. Barthelmes, A. Güntner, and M. Rothacher (2007), Towards a characterization of temporal gravity field variations in GRACE observations and global hydrology models, In proceedings of the 1st International Symposium Gravity Field Service, Harita Dergisi, General Command of Mapping, *73*(18).
Poveda, G., and O. J. Mesa (1997), Feedbacks between hydrological processes in tropical South America and large-scale ocean-atmospheric phenomena, *J. Climate*, *10*, 10.
Preisendorfer, R. W. (1988), *Principal component analysis in meteorology and oceanography*, Elsevier Science Publishers, Amsterdam.
Rajagopalan, B., and U. Lall (1998), Interannual variability in western US precipitation, *J. Hydrol.*, *210*, 1-4.
Reigber, C., R. Schmidt, F. Flechtner, R. König, U. Meyer, K. H. Neumayer, P. Schwintzer, and S. Y. Zhu (2005), An Earth gravity field model complete to degree and order 150 from GRACE: EIGEN-GRACE02S, *Journal of Geodynamics*, *39*, 1–10.
Rodell, M., et al. (2004), The Global Land Data Assimilation System, *Bull. Amer. Meteorol. Soc.*, *85*(3), 381–394.
Sasgen, I., Z. Martinec, and K. Fleming (2007), Wiener optimal combination and evaluation of the Gravity Recovery and Climate Experiment (GRACE) gravity fields over Antarctica, *J. Geophys. Res.*, *112*, L04401, doi:10.1029/2006JB004605.
Schmidt, R., et al. (2006), GRACE observations of changes in continental water storage, *Global and Planetary Change*, *50*, 112–126.
Schmidt, R., et al. (2007), GRACE Time-Variable Gravity Accuracy Assessment, in *Dynamic Planet, IAG Symposium 130, ISBN 3-540-49349-5*, edited by P. Tregoning and C. Rizos, pp. 237–243, Springer, Berlin.
Swenson, S., and J. Wahr (2006), Post-processing removal of correlated errors in GRACE data, *Geophys. Res. Lett.*, *33*, L08402, doi:10.1029/2005GL025285.
Tamisiea, M. E., J. X. Mitrovica, and J. L. Davis (2007), GRACE Gravity Data Constrain Ancient Ice Geometries and Continental Dynamics over Laurentia, *Science*, *316*, doi:10.1126/science.1137157.
Tapley, B. D., and C. Reigber (2001), The GRACE Mission: Status and Future Plans, *EOS Trans. AGU*, *82*(47), Fall Meet., Suppl. G41C-02.
Tapley, B. D., S. Bettadpur, J. C. Ries, P. F. Thompson, and M. M. Watkins (2004), GRACE Measurements of Mass Variability in the Earth System, *Science*, *305*, 503–506, doi:10.1126/science.1099192.
Velicogna, I., and J. Wahr (2006), Acceleration of Greenland Ice Mass Loss in Spring 2004, *Nature*, *443*, 329–331, doi:10.1038/nature.05168.
Wahr, J., M. Molenaar, and F. Bryan (1998), Time variability of the Earth's gravity field: Hydrological and oceanic effects and their possible detection using GRACE, *J. Geophys. Res.*, *103*, 30,205–30,230, doi:10.1029/98JB02844.
Wahr, J., S. Swenson, V. Zlotnicki, and I. Velicogna (2004), Time-variable gravity from GRACE: First results, *Geophys. Res. Lett.*, *31*, L11501, doi:10.1029/2004GL019779.
Wahr, J., S. Swenson, and I. Velicogna (2006), Accuracy of GRACE mass estimates, *Geophys. Res. Lett.*, *33*, L06401, doi:10.1029/2005GL025305.
Wilks, D. S. (1995), *Statistical methods in the atmosphere sciences: an introduction*, Academic Press, San Diego.
Zeng, N. (1999), Seasonal cycle and interannual variability in the Amazon hydrologic cycle, *J. Geophys. Res.*, *104*(D8), 9097–9106.
Zeng, N., J. H. Yoon, A. Mariotti, and S. Swenson (2008), Variability of basin-scale terrestrial water storage from a PER water budget method: The Amazon and the Mississippi, *J. Climate*, *21*, 248–265.

R. Schmidt, GeoForschungsZentrum Potsdam, Telegrafenberg, D-14473 Potsdam, Germany. (rschmidt@gfz-potsdam.de)

S. Petrovic, GeoForschungsZentrum Potsdam, Telegrafenberg, D-14473 Potsdam, Germany. (sp@gfz-potsdam.de)

A. Güntner, GeoForschungsZentrum Potsdam, Telegrafenberg, D-14473 Potsdam, Germany. (guentner@gfz-potsdam.de)

F. Barthelmes, GeoForschungsZentrum Potsdam, Telegrafenberg, D-14473 Potsdam, Germany. (bar@gfz-potsdam.de)

J. Wünsch, GeoForschungsZentrum Potsdam, Telegrafenberg, D-14473 Potsdam, Germany. (wuen@gfz-potsdam.de)

J. Kusche, GeoForschungsZentrum Potsdam, Telegrafenberg, D-14473 Potsdam, Germany. (jkusche@gfz-potsdam.de)

Table 1. Variances and cumulative variances (in %) from EOF analysis of GRACE-based data grids of surface mass anomalies for some drainage basins.

Mode No.	Continents		Amazon		Ganges		Mississippi	
	var	cum	var	cum	var	cum	var	cum
1	58.6	58.6	77.0	77.0	87.3	87.3	62.3	62.3
2	11.9	70.5	17.3	94.2	9.1	96.4	14.5	76.8
3	6.5	77.0	2.7	97.0	1.4	97.8	8.2	85.0
4	3.5	80.6	1.0	97.9	1.0	98.8	6.8	91.8
5	2.1	82.7	0.5	98.4	0.6	99.4	2.4	94.2

Table 2. Results of frequency analysis for grid points over all continents for GRACE – significant periods. Unit of period and phase is [days]. The unit of the amplitudes is relative.)

No.	Mode	Period T		Phase φ		Amplitude A		[%] of total
1	1	363.2	± 0.3	99.3	± 0.4	13.96	± 0.08	57.9
2	2	353.9	± 0.7	359.8	± 0.9	6.00	± 0.08	11.3
3	4	768.5	± 37.8	130.6	± 18.7	3.09	± 0.27	1.9

Table 3. Same as Table 2 but for WGHM – four strongest periods.

No.	Mode	Period T	Phase φ	Amplitude A	[%] of total
1	1	364.2	83.2	10.29	67.8
2	2	352.6	344.6	4.49	13.2
3	3	404.8	395.8	1.58	3.7
4	5	870.6	47.9	1.18	1.5

Table 4. Results of frequency analysis for grid points inside the Amazon basin for GRACE – significant periods. Unit of period and phase is [days]. The unit of the amplitudes is relative.

No.	Mode	Period T		Phase φ		Amplitude A		[%] of total
1	1	359.8	± 0.6	114.5	± 0.8	7.34	± 0.08	73.0
2	2	355.6	± 0.7	201.6	± 0.9	3.28	± 0.04	16.1
3	1	943.3	± 26.5	603.8	± 18.7	1.10	± 0.09	1.7
4	3	462.3	± 6.2	387.8	± 4.5	0.59	± 0.07	1.3
5	1	501.9	± 45.3	496.0	± 40.3	0.94	± 0.10	1.2

Table 5. Same as Table 4 but for WGHM – five strongest periods.

No.	Mode	Period T	Phase φ	Amplitude A	[%] of total
1	1	359.4	105.2	4.62	73.5
2	2	352.2	193.8	1.83	12.5
3	1	1036.6	440.8	1.01	4.4
4	1	485.6	466.6	0.97	2.4
5	1	272.1	136.7	0.54	1.3

Table 6. Results of frequency analysis for grid points inside the Ganges basin for GRACE – significant periods. Unit of period and phase is [days]. The unit of the amplitudes are relative.

No.	Mode	Period T		Phase φ		Amplitude A		[%] of total
1	1	362.7	± 1.0	265.1	± 1.4	2.69	± 0.06	79.0
2	1	183.4	± 1.0	57.9	± 2.3	0.71	± 0.05	4.6
3	2	352.7	± 5.1	358.6	± 13.2	0.60	± 0.06	4.6

Table 7. Same as Table 6 but for WGHM – three strongest periods.

No.	Mode	Period T	Phase φ	Amplitude A	[%] of total
1	1	362.1	254.2	2.06	90.0
2	1	181.5	56.9	0.55	4.8
3	2	179.3	53.5	0.20	1.1

Table 8. Results of frequency analysis for grid points inside the Mississippi basin for GRACE – significant periods. Unit of period and phase is [days]. The unit of the amplitudes are relative.

No.	Mode	Period T		Phase φ		Amplitude A		[%] of total
1	1	360.0	± 3.2	91.1	± 3.1	1.29	± 0.06	43.5
2	1	905.0	± 32.0	899.4	± 32.9	0.85	± 0.07	9.3
3	1	484.4	± 5.4	474.4	± 9.9	0.50	± 0.06	3.5

Table 9. Same as Table 8 but for WGHM – three strongest periods.

No.	Mode	Period T	Phase φ	Amplitude A	[%] of total
1	1	362.0	49.8	0.98	38.8
2	1	923.6	908.8	0.67	18.7
3	2	2114.5	380.1	0.61	18.0

Table 10. Same as Table 4 but for LaD, H96 and GLDAS – two strongest periods.

Model	No.	Period T	Phase φ	Amplitude A	[%] of total
H96	1	363.0	78.2	3.92	85.9
	2	359.5	166.3	1.36	10.4
LaD	1	362.1	80.5	4.70	78.9
	2	353.7	165.6	2.01	14.2
GLDAS	1	363.0	85.6	4.21	80.2
	2	358.8	170.6	1.68	12.4

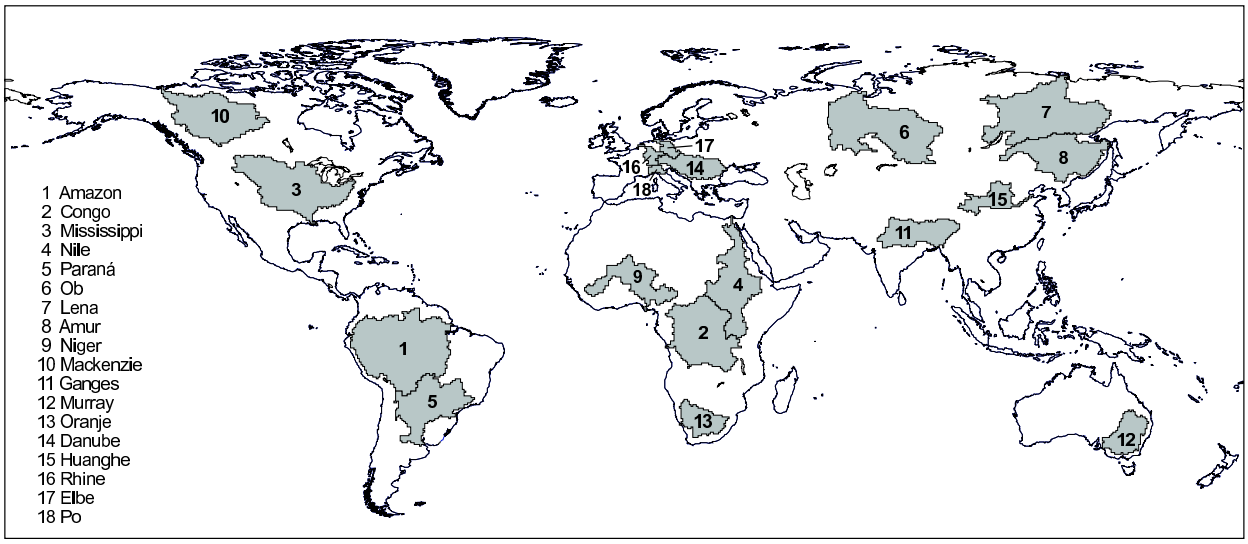

Figure 1. Location and distribution of 18 drainage basins investigated.

input: t_i, $y(t_i)$ $(i = 1, \ldots, N)$, ε

$n = 0$, $y_0(t_i) = 0$ $(i = 1, \ldots, N)$, $\varepsilon_n = 2\varepsilon$

$\varepsilon_n > \varepsilon$

- $z(t_i) = y(t_i) - y_n(t_i)$ $(i = 1, \ldots, N)$
- global optimization
  - find ω_{n+1} from $z(t)$
- use linearity
  - compute: B_{n+1}, C_{n+1}
- common adjustment (local optimization)
  - compute: A_0, D, $B_1, \ldots, B_{n+1}$, $C_1, \ldots, C_{n+1}$, $\omega_1, \ldots, \omega_{n+1}$
- n:=n+1
- compute: $y_n(t_i)$ $(i = 1, \ldots, N)$, ε_n

output: A_0, D, $B_1, \ldots, B_n$, $C_1, \ldots, C_n$, $\omega_1, \ldots, \omega_n$, ε_n

Figure 2. Sequential search algorithm for the determination of arbitrary periods.

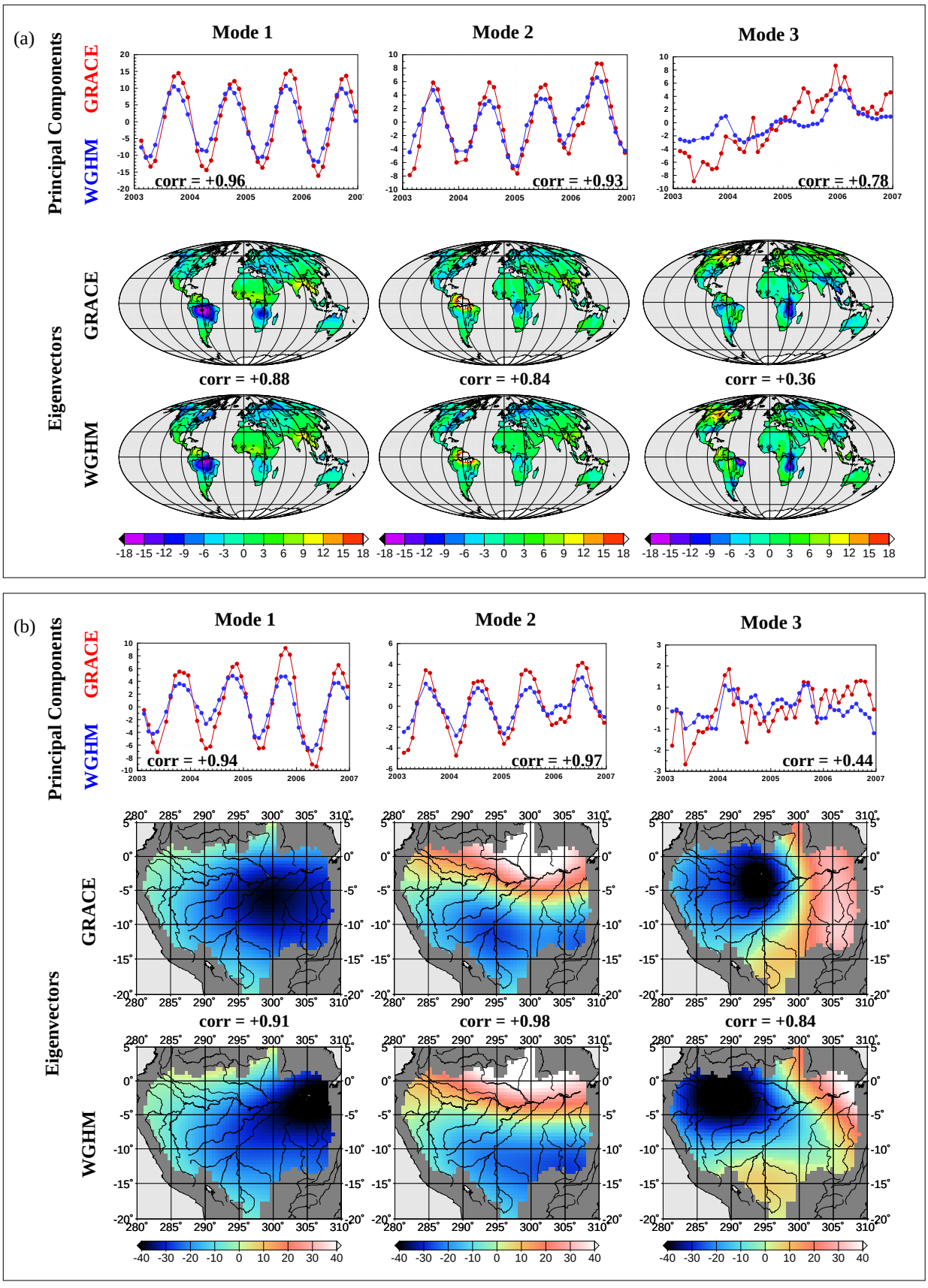

Figure 3. (a) Eigenvectors and principal components of the first three modes (left to right column) for the GRACE and the WGHM time series of grid points over continents. The values labeled *corr* give the correlation coefficients between the corresponding eigenvectors respectively the corresponding principal components. (b) Same as (a), however, EOF applied to grid points located within the Amazon basin.

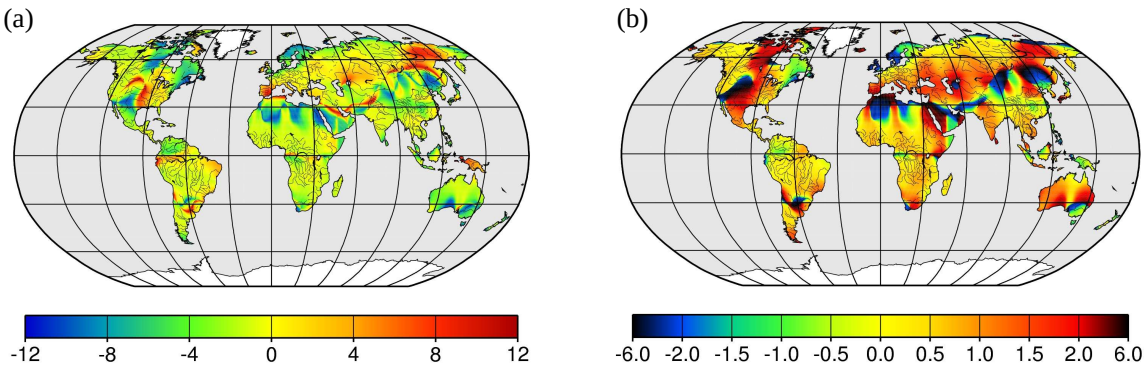

Figure 4. (a) Differences of pixel-wise annual periods derived from the annual harmonic terms found in GRACE versus corresponding terms found in WGHM. Units are days. (b) Same as (a) but for annual phases. Units are months.

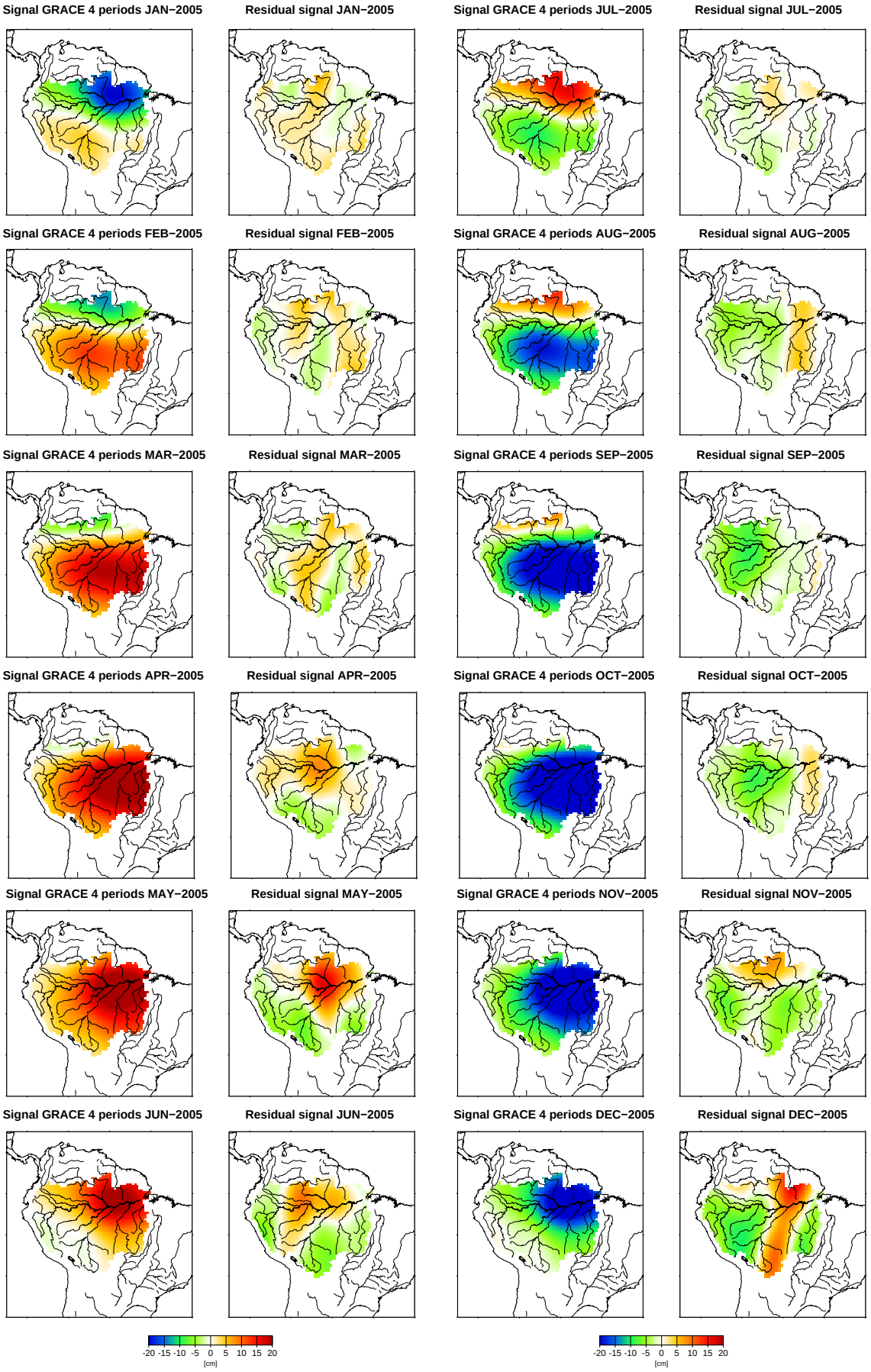

Figure 5. Synthesis of GRACE-based surface mass anomalies in the Amazon based on principal components replaced by the harmonic model of equation (2) based on the first four harmonic terms from Tab. 4. In the first and third column from left the reconstructed signal is shown for the months January to June 2005 and July to December 2005, respectively. The second and fourth column show the residual signal computed as the difference of the original GRACE data grid minus the reconstructed signal shown in columns one and three (from the left). Units: cm water column.

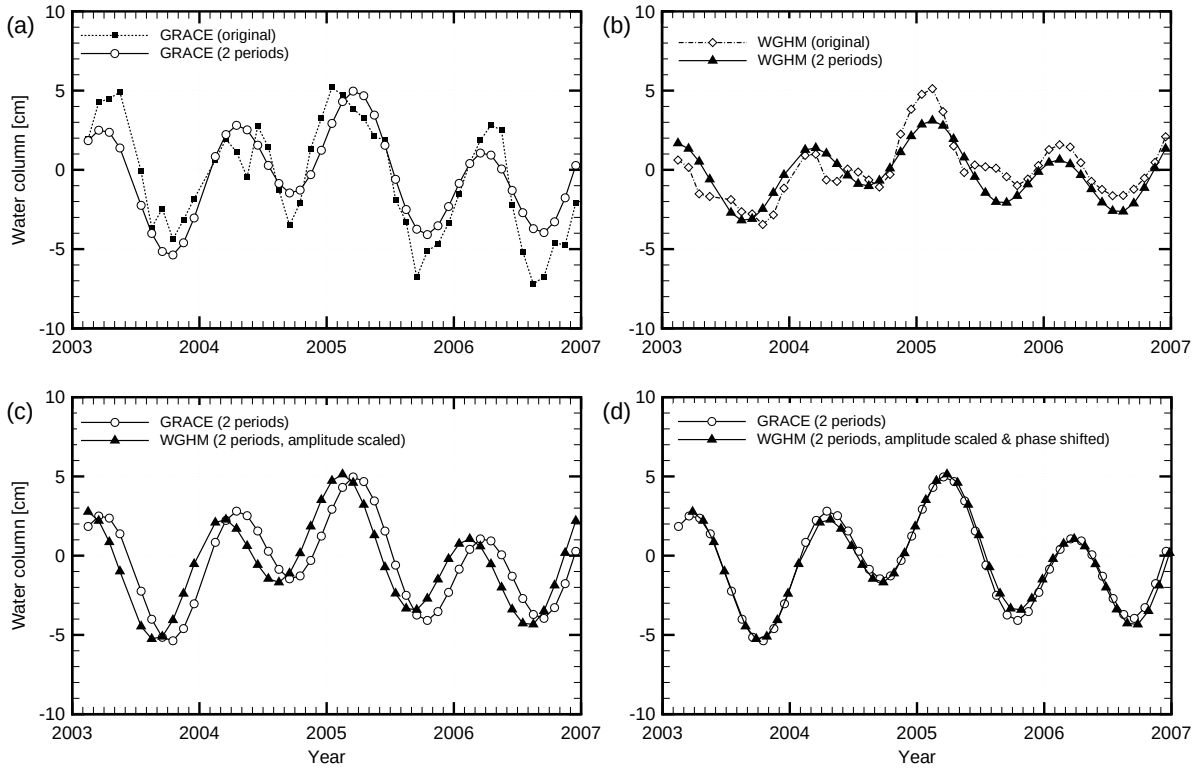

Figure 6. Time series of basin averages for the Mississippi basin from Gaussian averages of surface mass anomalies in terms of the equivalent height of a water column. Filter radius 500 km. Units cm. (a) The original data series and the reconstructed version for GRACE where the latter one is based on the annual and long-periodic harmonic terms displayed in Tab. 8. (b) Same as (a) but for WGHM. The harmonic terms for WGHM are taken from Tab. 9. (c) The reconstructed signals shown in (a) and (b), but the amplitude of the WGHM curve has been scaled to match the amplitude of the filtered GRACE signal curve. (d) The same as (c), however, the WGHM curve has been additionally shifted to match the filtered GRACE signal curve.